

Short Communication

Formation of CdS Nanoparticles in Microemulsion Using Different Co-surfactant and Water to Surfactant Molar Ratio

P. Sharma^{*1}, S. Singh², H. S. Virk¹

1- Nanotechnology Research Center, D.A.V. Institute of Engg. & Technology, Kabir Nagar, Jalandhar-144008, India

2- Department of Chemistry, Singhania University, Pacheri Bari, Jhunjhunu, 333575, India

(*) Corresponding author: chem.sharma@gmail.com

(Received: 27 Aug. 2010 and Accepted: 30 Nov. 2010)

Abstract:

Cadmium Sulphide (CdS) nanoparticles were prepared using microemulsion method using cadmium chloride as cadmium source and sodium sulphide as sulphur source. The obtained nanoparticles structures were characterized by X-ray diffraction (XRD) and Transmission Electron Microscopy (TEM) whereas optical characterization was done by Ultra Violet-Visible absorption. XRD result shows that CdS nanoparticles of hexagonal phase are formed. The TEM result indicates that the synthesized CdS nanoparticles are of variable morphology like spherical, cylindrical, nanorods and nanoneedles. Histograms help to evaluate size and aspect ratio of nanoparticles. UV-Visible spectroscopy reveals that as prepared CdS nanoparticles show a quantum confinement effect with shift in band gap. It is also found that water to surfactant molar ratio (wo) and co-surfactant are vital factors in the morphology and optical properties of CdS nanoparticles.

Keywords: *Microemulsion, nanoparticles, nanoneedles, nanorods, quantum confinement, molar ratio, co-surfactant, band gap shift.*

1. INTRODUCTION

In recent years, semiconductor nanoparticles have attracted much attention in both fundamental research and technical applications owing to their unique size dependent electronic [1-4], optical [5-7], catalytic [8-9], and electrochemical [10] properties compared to their bulk forms. Such behavior arises due to quantum size effects that are manifested only in the case of particles below a certain critical size limit [11]. Semiconductor nanoparticles that show these quantum size effects are called quantum dots. Since CdS

has 2.42 eV (515 nm) band gap, so it is most promising candidate among II-VI compounds for detecting visible radiation. As CdS has wide band gap, it is used as window material for hetero junction solar cells to avoid the recombination of photogenerated carriers which improves the solar cells efficiency [12]. CdS nanoparticles have various potential applications as optoelectronic devices [13-14], laser [15], photocatalysts [16], electrochemical cells [17], fluorescent labeling of cell organelles [18] etc. These exciting applications have been focused attention on the synthesis and size control of nanoparticles. Many synthetic methods have been used to prepare CdS

nanoparticles such as solid state reaction, Sol-gel process [19], sonochemical preparation [20], microwave heating [21], and photo etching [22]. In the past few years, CdS nanoparticles have been synthesized using various methods such as chemical precipitation method [23], using capping agents [24] and by facile synthesis using ethylenediamine [25] etc. but microemulsion synthesis [26] has been recently obtained nanoparticles with dimensions in 1-10 nm range. Microemulsion is an isotropic, thermodynamically stable dispersion of oil, water, surfactant and often co-surfactant, which is normally alcohol. Microemulsion is the co-existence of an excess water phase and the surfactant molecules which aggregate in the oil phase in the form of reverse micelle. It is well known that these micelles could perform as nano-scaled reactors [27]. Once two microemulsions of which one contains the precursor and the other contains the precipitating agent are uniformly mixed, the reaction will occur in controlled manner in the micelles which have the size in order of nanometers, resulting in the formation of nanoparticles of controlled characteristics. It is also known that addition of co-surfactant especially low molecular weight alcohols can reduce the surfactant concentration in microemulsion preparation. The amphiphilic nature of co-surfactant could also enable them to distribute between the aqueous and oil phase [28]. In our investigation, we have employed microemulsion technique and synthesized CdS nanoparticles with different co-surfactants and w_o .

2. EXPERIMENTAL DETAILS

2.1. Materials

Cadmium Chloride (CdCl_2), Sodium Sulphide (Na_2S), Cyclohexane, n-butanol, n-hexanol and cetyltrimethylammoniumbromide (CTAB) used in this experiment are of analytical grade and used without any further purification. De-ionized water was used for sample preparation.

2.2. Synthesis of CdS nanoparticles

The four-solvent reverse micelle system reported elsewhere [29] was prepared by adding in sequence of 15 ml cyclohexane, 4.20 gm surfactant (CTAB), 2.5ml of 0.1M aqueous $\text{Na}_2\text{S}\cdot 9\text{H}_2\text{O}$ and $\text{CdCl}_2\cdot 5\text{H}_2\text{O}$, 3.5ml n-butanol and n-hexanol as co-surfactants whereas w_o (water to surfactant ratio) was kept 5 and 10. Solution was mixed vigorously at approximately 3000 rpm for 15 min. The same experiments with these surfactants were also performed by replacing $\text{Na}_2\text{S}\cdot 9\text{H}_2\text{O}$ with $\text{CdCl}_2\cdot 5\text{H}_2\text{O}$ of equal molarity. Then an equal volume of two microemulsions with the same surfactant, one containing S^{2-} and the other containing Cd^{2+} , was mixed together followed by gentle shaking for another 3 min. The final solution was let to settle at room temperature for 12 h to allow for the formation of nanomaterials with different morphologies. The precursor precipitate was separated in a superspeed centrifuge at 10000 rpm for 10 min. The precipitate was then washed in a 1:1 mixture of methanol and chloroform followed by 100% methanol to remove residual cyclohexane and surfactant from the particles. The particles were then dried at 100°C .

2.3. Method

The optical absorption spectra of as prepared samples were carried out by dispersing CdS powder in DMSO and ultrasonicate to determine bandgap and particles size using (UV-Thermoevolution) spectrometer in the wavelength range of 200-850 nm. Transmission Electron Microscopy (TEM) studies were performed using (HRTEM, Hitachi, H7500) with accelerating voltage 80kV for surface morphology and particle size determination. For TEM analysis, CdS nanoparticle powder were dispersed in acetone and ultrasonicated for 10 min. and then a drop of solution was taken on a carbon coated copper grid and dried for TEM analysis.

The dried CdS powder was used to characterized XRD pattern by X-Ray Diffractometer (X'Pert PRO PAN analytical, Netherland) with $\text{CuK}\alpha$ radiation source of $\lambda=1.5406 \text{ \AA}$, operated at 45kV for structural and phase analysis.

3. RESULT AND DISCUSSION

In order to investigate the effect of co-surfactant, n-butanol and n-hexanol were selected and added individually into different microemulsion system with concentration ratio of CTAB/Co-surfactant=1 while w_o were varied with the variation of 5, and 10. The reactant concentration was kept constant at 0.1 mol/dm³. All synthesis work was conducted at room temperature.

3.1. X-Ray Diffraction analysis

It has been observed that CdS nanoparticles display both cubic and hexagonal structures depending upon the synthesis technique used. Phase transition from cubic to hexagonal occurs due to

thermal annealing with resultant band gap shift in CdS. It is very difficult to differentiate the cubic from the hexagonal because the cubic (111) and the hexagonal (002) main peaks almost overlap, coinciding within 1%. Patterns corresponding to the hexagonal phase show a preferred orientation along the (002) direction. It has been reported that CdS nanoparticles are also produced in β -phase of cubic crystal system with (111) main peak in XRD spectrum. XRD spectra of CdS nanoparticles synthesized in our experiments reveals 12 peaks corresponding to miller indices (100), (002), (101), (102), (103), (200), (112), (201), (202) and (203) as shown in Figure 1. The spectrum shows five prominent peaks at $2\theta=24.8671$, 26.5687, 28.2424, 43.8178 and 51.9481 corresponding to Miller indices (100), (002), (101), (110) and (112) respectively. The most prominent peak at

Table 1: Assignment of Miller Indices to CdS nanocrystals.

Sr. No.	Pos. [$^{\circ}2\theta$.]	d-spacing [\AA]	hkl
1.	24.8671	3.58064	100
2.	26.5687	3.35506	002
3.	28.2424	3.15991	101
4.	43.8178	2.06613	110
5.	51.9481	1.76028	112

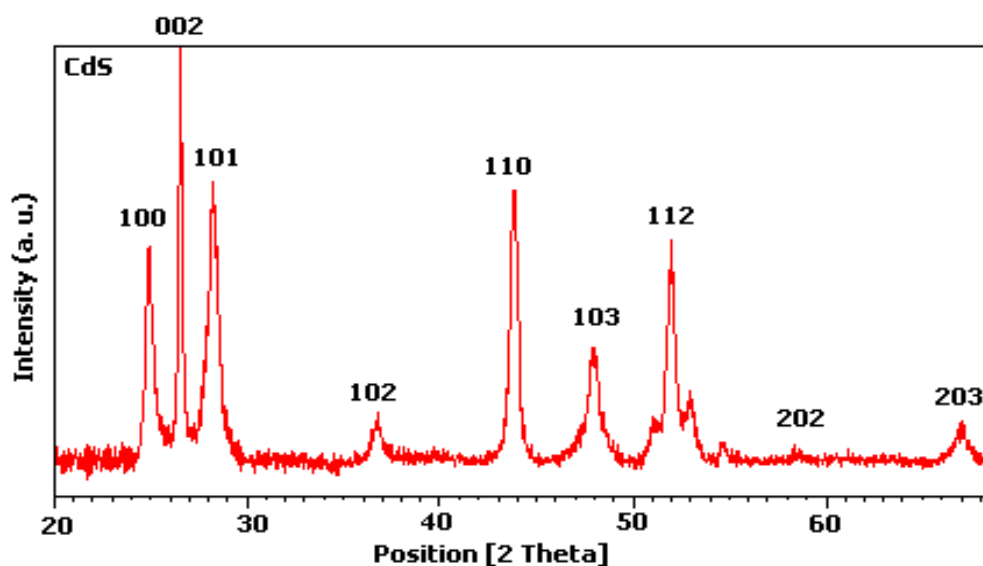


Figure 1: XRD of typical CdS nanoparticles samples obtained from w/o microemulsion

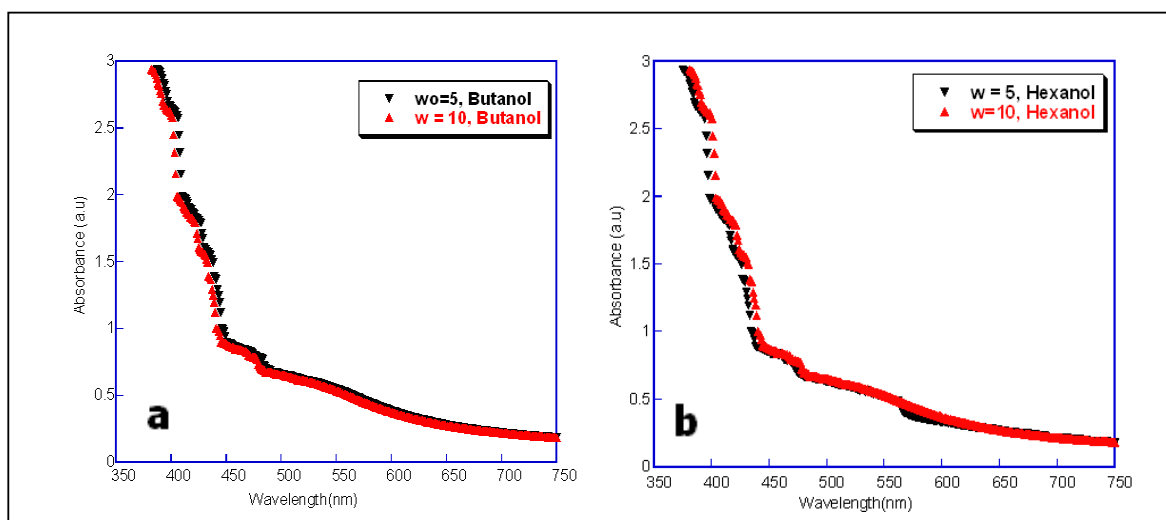


Figure 2: Absorption spectra as a function of wavelength at $w_o = 5$ and 10 (a) *n*-butanol (b) *n*-hexanol

$2\theta=26.5687$ corresponds to *hkl* (002) with lattice constants of $a=4.14\text{ \AA}$ and $c=6.72\text{ \AA}$. All the peaks can be indexed to hexagonal CdS, consistent with the literature data of JCPDS 41-1049 card. It clearly shows that CdS nanoparticles crystallize in hexagonal structure. Table 1 summarizes the XRD analysis result of some prominent CdS peaks, which were compared with the standard diffraction pattern (JCPDS 41-1049). XRD spectra do not show any peaks of impurities, which indicates the high purity of the product.

3.2 UV-Visible analysis

Figure 2(a,b) show the absorption spectra for the CdS nanoparticles (in CTAB/isooctane/different co-surfactant i.e *n*-butanol and *n*-hexanol) for w_o ratio of 5 and 10 as compared to the band gap of bulk CdS 2.42 eV, the absorption spectra clearly show a blue shift due to the quantum confinement effect. The absorption edge shifting to large wavelength region with increase in value of w_o . The optical spectra of the CdS particles formed indicate that the particles formed are in

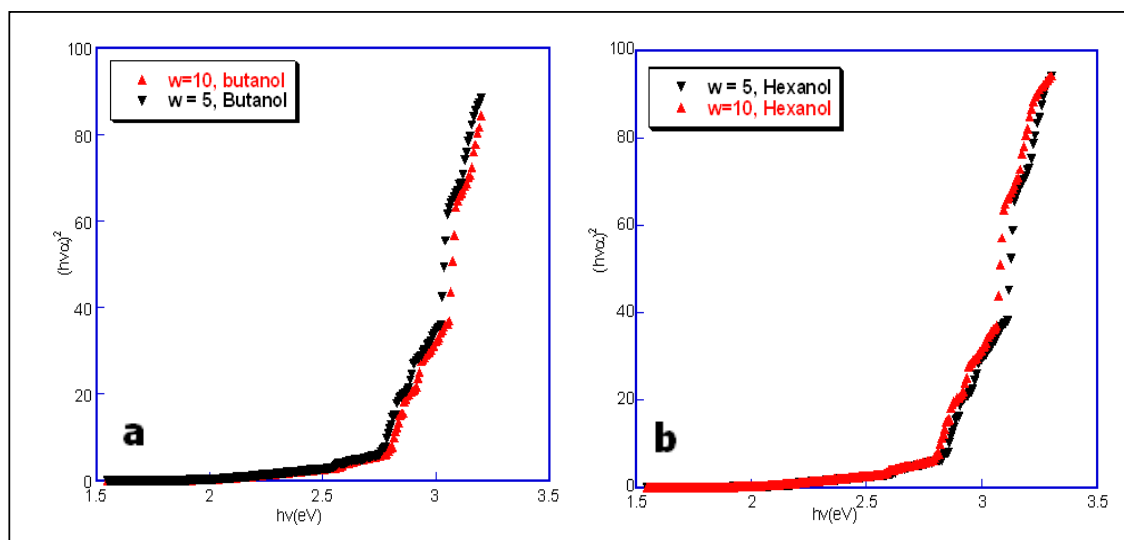


Figure 3: Plot of $(h\nu\alpha)^2$ versus $(h\nu)$ at $w_o = 5$ and 10 (a) *n*-butanol (b) *n*-hexanol.

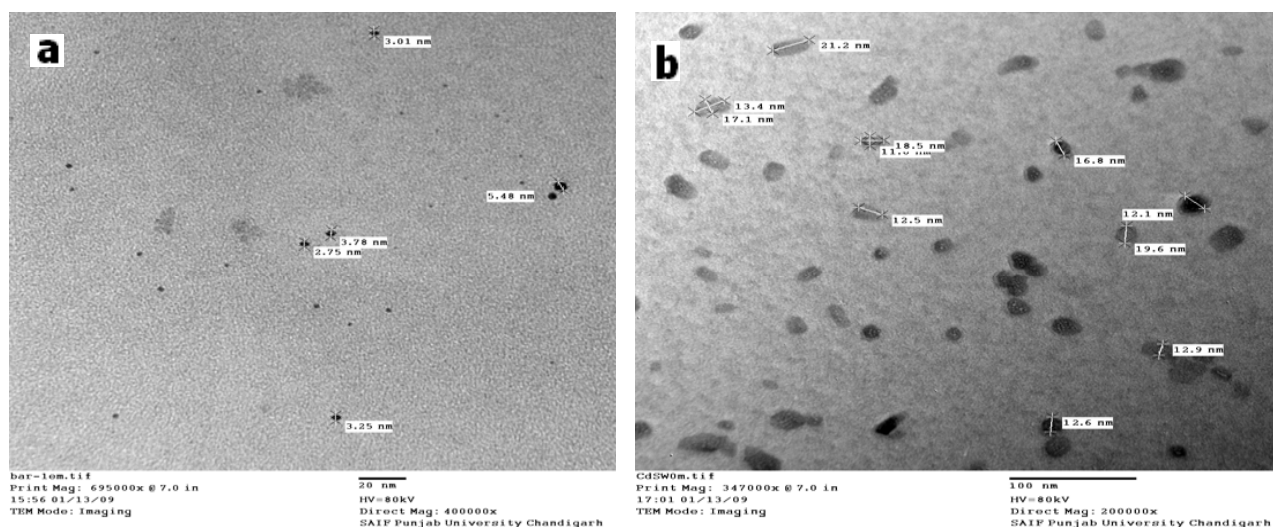


Figure 4: TEM image of CdS nanoparticles synthesized in microemulsion with *n*-butanol as a co-surfactant at (a) $w_o = 5$, mean dia.=3.65nm (b) $w_o = 10$, mean dia.=14.42nm

the nanoparticle regime. Band gap values were obtained from the linear fit for $(h\nu\alpha)^2$ versus $(h\nu)$ plot shown in Figure 3(a,b) for $w_o=5$ and 10. The band gap of the CdS nanoparticles is a function of size under tight binding approximation (TBE) as well as effective mass approximation (EMA). TBA fits better for particles with diameters smaller than 4nm whereas EMA fits for all range of sizes. [25] The relationship between the particle size and band gap is given by equation (1).

$$E_g = E_g(0) + \alpha/d^\beta \quad (1)$$

where $E_g(0)$ is band gap of bulk CdS (2.42eV), α and β being constants. The value of $\beta=2$ for effective mass approximation [30]. EMA fitted to the above relation and the values of α and β were obtained as 13eV/nm² and 2, respectively from the data taken from Lippens and Lannoo [31] for the relationship between band gap and particles size. The band gap values of the nanoparticles formed with different co-surfactants

Table 2: Band gap values and particles sizes of CdS nanoparticles formed at $w_o=5, 10$ with *n*-butanol and *n*-hexanol as co-surfactants.

Co-surfactant	Molar ratio (w_o)	UV-Visible		TEM
		Band Gap (eV)	Particle Size (nm)	Mean Particle Size (nm)
n-butanol	$w_o = 5$	2.77	6.05	3.65
	$w_o = 10$	2.72	6.25	14.42
n-hexanol	$w_o = 5$	2.85	5.49	10.81
	$w_o = 10$	2.75	6.27	10.05

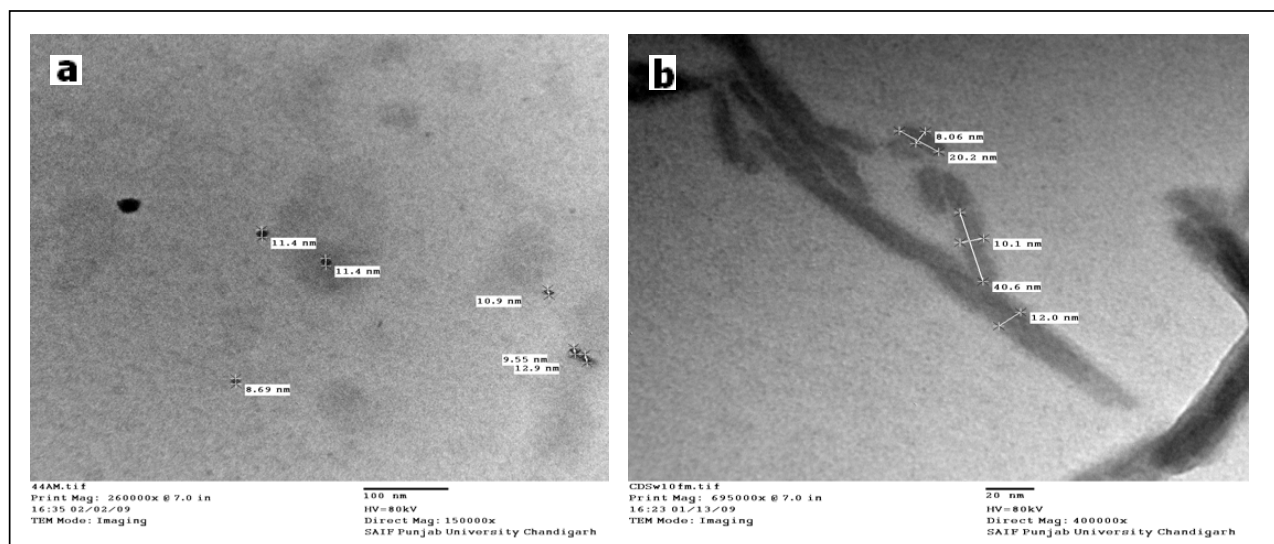


Figure 5: TEM image of CdS nanoparticles synthesized in microemulsion with n-hexanol as a co-surfactant at (a) $w_o = 5$, mean dia. = 10.81nm (b) $w_o = 10$, mean dia. = 10.05

and w_o along with the particles size estimated using equation (1), are given in the Table 2.

But for accurate size assessment by UV-Visible absorption spectroscopy [32], particles should be exactly spherical in shape. But it is evident from TEM images that most of the particles of various samples are not spherical in shape. We believe that due to non-spherical shape, exact size determination by absorption spectroscopy is not possible and only the approximate particle size calculation could be obtained from this study, whereas TEM images give a better assessment.

3.3. TEM analysis

By employing n-butanol as co-surfactant at relatively low $w_o=5$, TEM image in Figure 4(a) shows that the synthesized products consists of uniform nanoparticles or quantum dots with mean diameter of 3.65 nm. The smaller size of quantum dot leads their higher efficiency of light emission and because of this, it is reasonable to expect that the synthesized product could potentially be used in electroluminescent applications upon doping.

Figure 4(b) shows elliptical shaped nanoparticles

with mean diameter of 14.42nm at $w_o=10$. Similarly, using hexanol, at $w_o=5$ spherical nanoparticles with mean diameter of 10.81nm size are formed. However, significant morphological change is observed at $w_o=10$, where instead of spherical nanoparticles, nanoneedles with mean diameter of 10.05 nm are formed (Figure 5b).

It should be noted that there were some significant changes in the morphology of the synthesized CdS nanoparticles when different co-surfactants were used. At $w_o=5$, comparison of Figures 4(a) and 5(a) reveals that spherical nanoparticles are formed in both cases. However, comparing Figures 4(b) and 5(b) at $w_o=10$, significant morphological change were observed with n-butanol and n-hexanol where elliptical shaped nanoparticles and nanoneedles were formed, respectively instead of spherical nanoparticles.

4. CONCLUSION

CdS nanoparticles prepared by microemulsion, show interesting morphology which were synthesized in quaternary w/o microemulsion

systems using different co-surfactants. It is clearly shown by TEM images that the size and the morphology of CdS nanoparticles are dependent on the nature of co-surfactant and water to surfactant molar ratio (w_o). Co-surfactant with larger molecular size such as n-hexanol could provide higher possibility to synthesize CdS nanoparticles with high aspect ratio like nanoneedles or nanorods. However, observable morphological change is observed at $w_o=10$. The elliptical nanoparticles formed using n-butanol as a co-surfactant is replaced by long nanoneedles using n-hexanol. Optical absorption spectra also supports the results as band gap shifts are observed at $w_o=5$ and 10 using different co-surfactants. However exact size assessment is not possible by absorption spectra due to non spherical shape of nanoparticles, the evidence for which is provided by TEM images.

ACKNOWLEDGEMENTS

The authors wish to express their gratitude to the Principal DAV institute of Engineering & Technology, Jalandhar, India and DAV Managing Committee, New Delhi for providing research grants for setting up Nanotechnology Research Center. They are thankful to Dr. Rajeev Sharma, Department of Chemistry, DAV College, Jalandhar, India for UV-Visible analysis.

REFERENCES

1. A. Henglein, Chem. Rev. 89, 1861, (1989).
2. M. L. steigerwald and L. E. Brus, Acc. Chem. Res. 23, 183, (1990).
3. Y. Wang and N. Herron, J. Phys. Chem. 95, 525, (1991).
4. H. Weller, Angew. Chem., Int. Ed. Engl. 32, 41, (1993).
5. Y. Wang, Acc. Chem. Res. 24, 133, (1991).
6. E. Rosencher, A. Fiore, B. Vinter, V. Berger, P. Bois and J. Nagle, Science. 271, 168, (1996).
7. M. A. Hines and P. Guyot-Sionnest, J. Phys. Chem. B 100, 468, (1996).
8. A. J. Bard, Science, 207, 4427, (1980).
9. S. Yanagida, M. Yooshiya, T. Shiragami, C. J. Pac, H. Mori and H. Fujita, J. Phys. Chem. 94, 3104, (1990).
10. S. K. Haram, B. M. Quinn and A. J. Bard, J. Am. Chem. Soc., 123, 8860, (2001).
11. L. E. Brus, J. Chem. Phys. 80, 4403, (1984).
12. Arturo Morales-Acevedo, Solar Energy Materials and Solar Cells 90, 2213 (2006).
13. V. L. Colvin, M. C. Schlamp and A. P. Alivisatos, Nature. 370, 354 (1994).
14. B. O. Dabbousi, M. G. Bawendi and O. Onitsuka, Appl. Phys. Lett. 66, 1316, (1995).
15. L. Pavesi, L. D. Negro, C. Mazzoleni, G. Franzo and F. Priolo, Nature. 408, 440, (2000).
16. C. K Graetzel and M. Graetzel, J. Am. Chem. Soc. 101, 7741, (1979).
17. A. Hagfeldt and M. Graetzel, Chem. Rev. 95, 49, (1995).
18. Jr M. Bruchez, M. Moronne, P. Gin, S. Weiss and A. P. Alivisatos, Science. 281, 2013, (1998).
19. R. S Mane, and C. D. Lokhande, Mater. Chem. Phys. 1, 65, (2000).
20. G. Henshaw, I. P.Oarkin, and G. Shaw, Chem. Commun. 27, 1096, (1996).
21. Y. Wada, H. Kuramoto, J.Anand, T. Tikamura, T. Sakata, H. Mori, and S. Yanagida, J. Mater. Chem. 11, 1940, (2001).
22. T. Torimoto, H. Kontani, Y. Shibutani, S. Kuwabata, T. Sakata, H. Mori, and H. Yoneyama, J. Phys. Chem. 105, 6838, (2001).
23. A. Guinier, X-ray diffraction. Freeman, San Francisco, CA. (1963).
24. V. Singh, P. Chauhan, Chalcogenide Letters, 6,421,(2009).

25. M. N. Kalasad, M. K. Rabinal and B. G. Malimani, *J. of Phys D: App Phys*, 43, 30, (2010).
26. M. Maleki, M. SasaniGhamsari, S. Mirdamdi, R. Ghasemzaheh, *Semiconductor Phys., Quantum Electronics & Optoelectronics*, 10, 30, 2007.
27. K. J. Klabunde (Ed.), *Nanoscale Materials in Chemistry*, Wiley-Interscience, New York. (2001).
28. R. G. Alany, T. Rades, S. Agatonovic-Kustrin, N.M. Davies, and I.G. Tucker, *Int. J. Pharm.* 196, 145, (2000).
29. K. Murakoshi, H. Hosokawa, M. Saito, Y. Wada, C. Sakata, H. Mori and S. Yanagida, *J. Chem. Soc. Faraday Trans.*, 94, 579, (1998).
30. X. H. Yang, Q. S. Wu, L. Lia, Y. P. Ding, G. X. Zhang, *Colloids and Surfaces A: Physicochem. Eng. Aspects* 264, 172, (2005).
31. V. A. Singh, V. Ranjan, V. Kumar, and S. K. Aggarwal, *Physics of Semiconductor Devices*, Narosa Publishing House. 69, (1998).
32. P. E. Lippens, and M. Lannoo, *Phys. Rev. B* 39, 1035, (1989).
33. J. J. Nanda et al., *Material Research Society*. 796, (2004).